*J. Electrochem. Sci. Eng.* **12(6)** (2022) 1165-1177; http://dx.doi.org/10.5599/jese.1531

Open Access : : ISSN 1847-9286
https://pub.iapchem.org/ojs/index.php/JESE

*Original scientific paper*

# Electrochemical determination of amaranth in food samples by using modified electrode

Sayed Zia Mohammadi[1], Yar-Mohammad Baghelani[2], Farideh Mousazadeh[3], Shamsi Rahimi[1] and Maryam Mohammad-Hassani[1,✉]

[1]*Department of Chemistry, Payame Noor University, Tehran, Iran*
[2]*Department of Chemistry, Faculty of Sciences, Ilam University, Ilam, Iran*
[3]*School of Medicine, Bam University of Medical Sciences, Bam, Iran*

*Corresponding authorc:* ✉*mohammadhassanipourm@gmail.com*

Received: September 23, 2022; Accepted: October 5, 2022; Published: November 4, 2022

***Abstract***

*In this paper, a new electrochemical sensor was reported for the determination of amaranth in drink soft. In this sensor, activated carbon-$Co_3O_4$ nanocomposite (AC-$Co_3O_4$) was employed as electrode modifying material. High pores of the activated carbon favour an access of aramanth nolecules within the pores of the working electrode surface, and allow fast electron transfer that is beneficial for the electrochemical detecion process. Thus, the electrochemical signal is obviously enhanced at AC-$Co_3O_4$ modified electrode compared to bare carbon paste electrode, and exhibited a wide linear response ranging from 0.1-215 μM with a low detection limit of 10.0 nM (based on $3S_b$/m). This work offers a new route in developing new electrochemical sensors for the determination of collorant additives and other hazard components in drink soft.*

**Keywords**

Electrochemical sensor; carbon paste electrode; activated carbon-$Co_3O_4$ nanocomposite

## Introduction

Bright colors make foodstuffs and soft drinks more attractive and appealing [1]. Therefore, various edible colorants, including natural colorants and artificial colorants are widely used in the food processing industry [2]. Because of charming color uniformity, excellent water solubility, cheap production cost, low microbiological contamination as well as high stability to light, oxygen and pH, synthetic colorants especially azo dyes have been widely used in food industry to improve the appearance and color of food products [3].

Amaranth, a typical synthetic azo colorant, has been extensively applied to give fascinating red color and make food more attractive and appealing. However, excessive intake of amaranth may cause adverse health effects such as dizziness, anxiety, allergic reaction, and even cancer [1,4-6]. Therefore, many countries have strictly regulated the additive dosage of amaranth. For example, in

both the USA and Japan, the use of amaranth has been voluntarily restricted in foodstuffs and beverages [7] and in China, amaranth is permitted to be added into some foodstuffs [8]. The World Health Organization has set the acceptable daily intake of amaranth as 0.5 mg $kg^{-1}$ [9]. Therefore, the content of amaranth in foods must be severely controlled and the detection of amaranth in a rapid, sensitive, simple, and cost-effective manner is paramount for human health and food safety.

Recently, various methods such as thin layer chromatography [10], high-performance liquid chromatography mass spectrometry [11,12], liquid chromatography-tandem mass spectrometry [13,14], spectrophotometry [15,16] and electrochemical analysis [17-21] have been reported to determine amaranth. Among those methods, electrochemical methods are more attractive than others because of their unique advantages such as low-cost, simple equipment and operation, quick response and ease of miniaturization [22-33]. Various electrochemical sensors have been successfully designed for detecting amaranth in foodstuffs and soft drinks [1,3,34-40].

The nanomaterials have excellent catalytic and electronic traits to convert biorecognition processes into electrochemical reaction, and also have the high loading receptor molecules to synergistically amplify target reaction, as well as have large surface area to increase mass transport.

Herein, we developed novel activated carbon-$Co_3O_4$ nanocomposite-modified carbon paste electrode (AC-$Co_3O_4$-CPE) for the sensitive detection of amaranth in foodstuffs. As far as we know, there was no report on the amaranth oxidation with the AC-$Co_3O_4$-CPE. Then, it was investigated for amaranth voltammetric detection in the real samples.

## Experimental

### *Instruments and chemicals*

Instruments utilized in this research are similar to the devices reported in the previous article [30]. Amaranth, cobalt chloride hexahydrate, $Na_2HPO_4$ and $NaH_2PO_4$ were Sigma-Aldrich (St. Louis, USA) and the rest reagents with analytical grades were also Sigma and thus applied with any additional treatments. Moreover, we employed $Na_2HPO_4$ and $NaH_2PO_4$ for preparing phosphate buffer (PBS) supporting electrolyte solution. Notably, we used deionized water to prepare all solutions freshly.

### *Fabrication of AC/$Co_3O_4$ nanostructure*

The AC-$Co_3O_4$ nanocomposite has been synthesized according to the previous report [41]. Briefly, five-gram $CoCl_2 \times 6H_2O$ was poured into ethanol solution (40 mL) plus activated carbon (5 g), followed by adding 12.5 mL of hydrazine hydrates (50 % $N_2H_4 \times H_2O$) and 12.5 g of sodium hydroxide (NaOH) as dropwise with vigorously stirring at an ambient temperature. Then, the produced AC-$Co_3O_4$ was collected, rinsed using the deionized water and the ethanol to exclude additional hydrazine. Drying the AC-$Co_3O_4$ has been performed in the oven for 4 hours at 90 °C.

### *Preparation of electrode*

100 mg of AC-$Co_3O_4$ nanocomposite and 900 mg graphite was mixed using a mortar for 10 min, and then 0.7 mL of paraffin was added to it and remixed for 10 min. Then, the resultant paste inserted into a glass tube (length = 10 cm; inner diameter = 3.4 mm) and packaged and then put a copper wire in the electrode for establishing an electrical contact. After that, we pressed additional paste out of the glass tube and used a weighing paper to polish it for obtaining the surface. The resulting electrode is displayed with AC-$Co_3O_4$-CPE.

Furthermore, the bare CPE without any AC-$Co_3O_4$ nanocomposite was constructed for comparison.

*Preparation process of the real samples*

Food samples including grape soda and Lemon soda were provided by a local supermarket. The liquid samples were transferred into beaker and degassed in an ultrasonic bath. Then 1.0 mL of the samples was pipetted into the voltammetric cell, and diluted to 10 mL with 0.1 M PBS (pH 7).

## Results and discussions

*Characterization of AC/$Co_3O_4$*

The morphology of AC/$Co_3O_4$ nanocomposite was examined by the scanning electron microscope (SEM) (Tescan, Czech Republic) images and the results was given in Fig 1. As can be seen, the AC/$Co_3O_4$ has an even nano-flower-shape morphology that is assembled through nano-sheets, thereby causing an elevation in the activated carbon surface area that shows a highly efficient surface area for electron transfer.

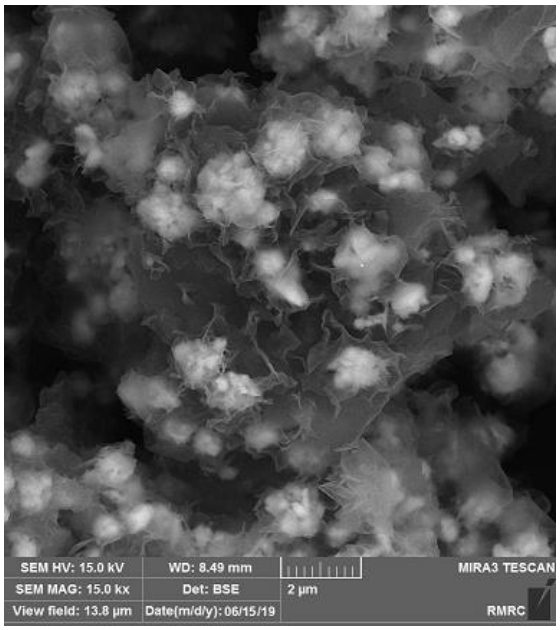


***Figure 1.*** *SEM image of AC/$Co_3O_4$ nanocomposite*

Figure S-1 (given in the Supplementary material) shows the Fourier Transform – infra red (FT-IR) (Bruker, Germany) spectra obtained for the functional groups of AC-$Co_3O_4$ nanocomposite. As seen, the bands at 3416 and 3445 $cm^{-1}$ correspond to O–H stretching related to the water molecule adsorption. The bands from 2850 to 2950 $cm^{-1}$ stand for the C-H stretching, the bands at 1623 and 1703 $cm^{-1}$ for carbonyl stretching vibration and carboxylic group [42]. The peak 1062 $cm^{-1}$ stands for C–O stretching vibration. The bands at 1000 to 1100 $cm^{-1}$ relate to C–O–C and C–O vibrations. The peak 2923 $cm^{-1}$ corresponds to $CH_2$ anti-symmetric and symmetric stretch vibrations. The peaks 435 and 564.47 $cm^{-1}$ show respectively metal oxygen (M–O) vibration bond in octahedral and tetrahedral locations, confirming the existence of cobalt oxide on the AC-$Co_3O_4$ surface [42].

XRD has been assessed using a diffractometer Bruker D8 ADANCE, having Cu Ka radiation. High angle X-ray diffractogram for the AC-$Co_3O_4$ nanocomposite are shown in Figure S-2. The diffraction peaks of $2\theta$ = 41.8, 44.4, 47.2, 51.9 and 76.0° (PDF# 15-0806) exhibit the typical metallic cobalt nano-particles (NPs) [42]. The amorphous structure of carbon is evident in a broad peak at $2\theta$ = 24° [42]. The calculation of particle size of cobalt NPs in the structure of AC-$Co_3O_4$ nanocomposite was performed in accordance with the diffraction peak ($2\theta$ = 44.4°) using the Scherrer equation and was 27.9 nm.

The X-ray photoelectron spectroscopy (XPS) (Tescan, Czech Republic) was applied to chemically determine the composition of AC-$Co_3O_4$ nanocomposite, whose spectra are shown in Figure S-3. The findings confirm the presence of O, Co, and C in the structure of AC-$Co_3O_4$ nanocomposite. The weight ratios of C (60.50 %), Co (28.72 %) and O (10.78 %) have been obtained having analyzed data quantitatively.

*Electrochemical behaviour of amaranth at the AC-$Co_3O_4$-CPE surface*

The CVs responses for the bare CPE and the AC-$Co_3O_4$-CPE in 0.1 M PBS (pH 7.0) containing 100.0 µM amaranth were presented in Figures 2a and 2b, respectively. As can be seen, potential of peak ($E_p$) for Amarant is 600 mV and 825 mV at the surface of AC-$Co_3O_4$-CPE and the bare CPE, which reflects the capability of AC-$Co_3O_4$ nanocomposite as good mediator. Compared to the unmodified electrode, the $E_p$ is shifted by about 225 mV to negative values. On the other hand, compared to the unmodified electrode, the peak current ($I_p$) in 100.0 µM amaranth solution (curve b) considerably elevated, which was caused by the probable electrocatalytic impacts of AC-$Co_3O_4$ nanocomposite on the amaranth.

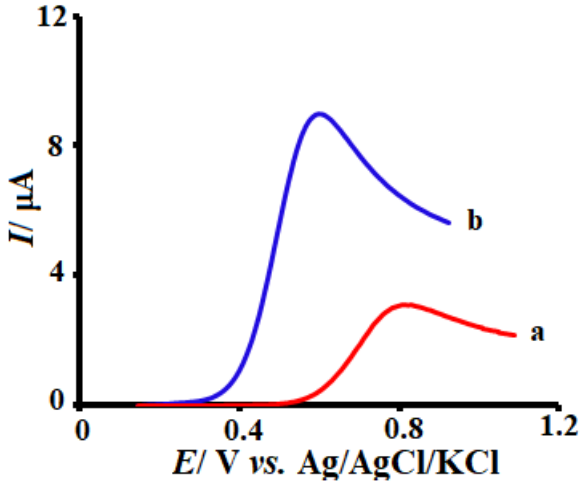


***Figure 2.*** *LSVs of the bare CPE (a) and the AC-$Co_3O_4$-CPE (b) in the presence of 100.0 µM amaranth in 0.1 M PBS (pH of 7.0). Scan rate = 50 mV $s^{-1}$ in all cases*

In the following, optimizing the solution pH would be crucial to achieve electrocatalytic oxidation of amaranth. Therefore, the dependence of electrochemical activity of amaranth on the pH value of the aqueous solution was also assessed. For this purpose, the CV used to investigate electrochemical activity of amaranth into 0.1 M PBS with different pH-values ($3.0 < pH < 9.0$) at the AC-$Co_3O_4$-CPE surface (Figure 3). The results showed that the electrochemical oxidation of amaranth at the AC-$Co_3O_4$-CPE surface in neutral conditions is better than acidic or alkaline conditions. Therefore, pH 7.0 was chosen as optimum pH for electrochemical oxidation of amaranth at the AC-$Co_3O_4$-CPE surface.

Additionally, the obtained results showed that with increase of pH, the peak potential ($E_p$) was shifted linearly to negative values (slope = 56.1 mV per unit of pH) that is close to the theoretical value (59.2 mV) and indicates that the number of protons and electrons involved in the oxidation process are equal [1,43,44]. With respect to these results, the possible oxidation mechanism of amaranth at the surface of AC-$Co_3O_4$-CPE was proposed in Scheme 1 that is in agreement with the proposed mechanism in the literature [1,43,44] and as can be seen, 2 electrons are involved in the oxidation of amaranth.

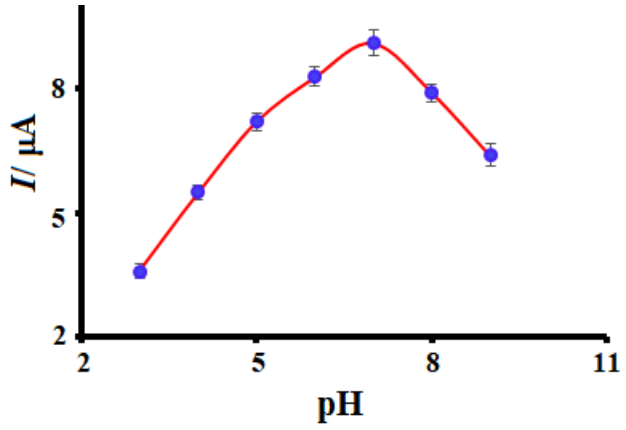


***Figure 3.*** *Variation of peak current of AC-$Co_3O_4$-CPE in 0.1 M PBS containing 100.0 µM aramanth with different pH values (3 to 9)*

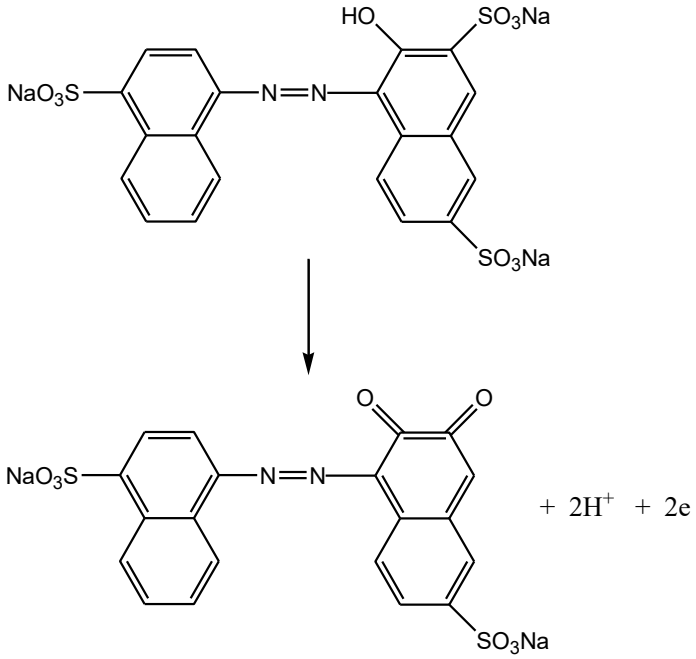


***Scheme 1.*** *Electro-oxidation of amaranth at the surface of AC-$Co_3O_4$-CPE*

In order to illustrate that the AC-$Co_3O_4$ nanocomposite could increase the electrode surface area in comparison to the surface of bare CPE, real surface area of AC-$Co_3O_4$-CPE and bare CPE were determined by the Randles-Sevcik (Eq. 1) [45]:

$$I = 2.69\times10^5 ACD^{1/2}n^{3/2}v^{1/2} \quad (1)$$

were $A$ is the effective surface area of each electrode ($cm^2$), $n$ is the number of electrons taking part in charge transfer process, $D$ is the diffusion coefficient of the analyte in the solution and $C$ is the concentration of the analyte in the solution. The values of $n$ and $D$ for $K_3Fe(CN)_6$ are 1 and $7.6\times10^{-6}$ $cm^2\,s^{-1}$ respectively.

The results showed that the real surface area of AC-$Co_3O_4$-CPE and bare CPE were 21.42 and 0.10 $cm^2$, respectively. Therefore, as expected, the surface area of AC-$Co_3O_4$-CPE increases with the addition of AC-$Co_3O_4$ nanocomposite to the matrix of the carbon paste.

In the following, the effect of scanning speed on the peak current ($I_p$) of amaranth was studied using linear sweep voltammetry (LSV) (Figure 4). The observations showed that the higher the scan speed, the higher $I_p$ and the $E_p$ shifted towards higher positive potentials. As can be seen (Inset of Figure 4), the $I_p$ *vs.* the square root of the scanning rate ($v^{1/2}$) varied linearly, therefore, the oxidation process of amaranth at the surface of AC-$Co_3O_4$-CPE is controlled by diffusion [45].

In the next step, the LSV obtained at the scan rate of 10 mV $s^{-1}$ was used for draw the TOEFL diagram (Figure 5). The ascending part of the voltammogram is called the Tafel region that under the influence by the electron transfer kinetic between amaranth and the AC-$Co_3O_4$-CPE.

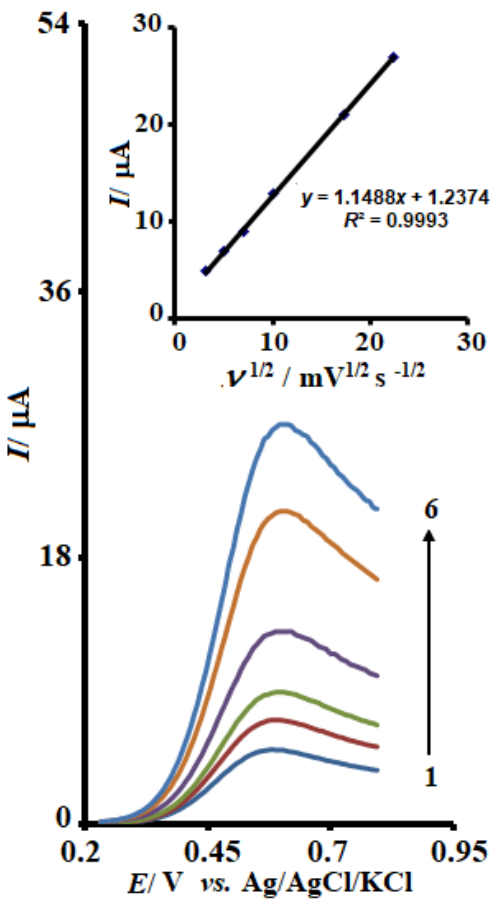


***Figure 4.*** *LSVs of AC-$Co_3O_4$-CPE in 0.1 M PBS (pH 7.0) containing 100.0 µM amaranth at various scan rates; numbers 1 - 6 correspond to 10, 25, 50, 100, 300 and 500 mV $s^{-1}$, respectively; inset: changes in the anodic peak current versus square root of scan rate*

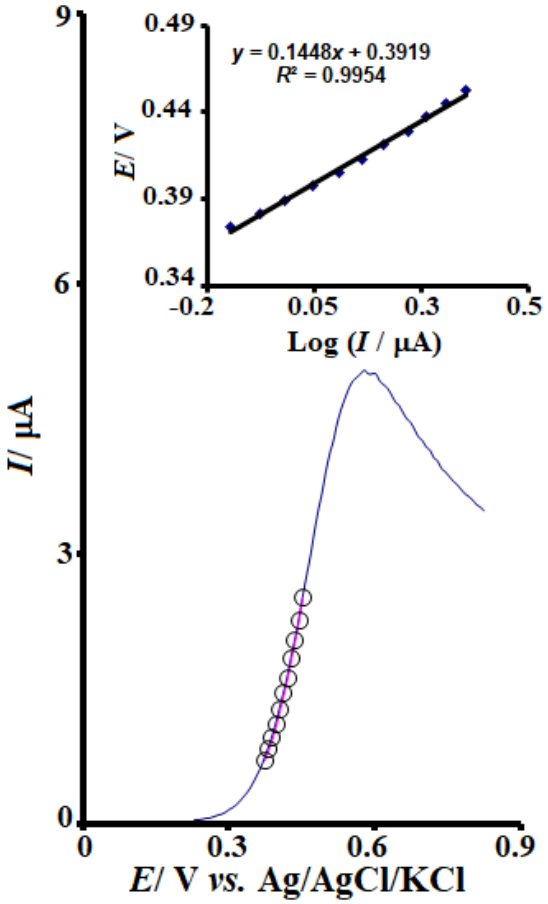


***Figure 5.*** *LSV of AC-$Co_3O_4$-CPE in 0.1 M PBS (pH 7.0) containing 100.0 µM amaranth at the scan rate of 10 mV $s^{-1}$. The inset exhibits the LSV-derived Tafel plot*

Due to the slope of the Tafel curve, which corresponds well to the involvement of 1 electron in the electrode rate-determining step [45], a charge transfer coefficient ($\alpha$) of 0.6 was obtained for amaranth.

*Chronoamperometric study*

In the following, to perform the chronoamperometric measurements of amaranth at the surface of the AC-$Co_3O_4$-CPE, the working electrode potential was adjusted at 650 mV (Figure 6). The current obtained from electrochemical reaction at the mass transport limited condition for electroactive material (in this case: amaranth), that having a diffusion coefficient $D$ can be ascribed by Cottrell equation (2) [45]:

$$I = nFAD^{1/2}C_b\pi^{-1/2}t^{-1/2} \quad (2)$$

where $D$ imply the diffusion coefficient ($cm^2$ $s^{-1}$) and $C_b$ the bulk concentration (mM). Chrono-amperometric measurements of aramanth were performed in diverse concentrations of amaranth (0.1 M of PBS at pH 7.0). Then, the plots of $I$ versus $t^{-1/2}$ were plotted (Figure 6a). In the next step, the

slopes of the obtained straight lines were plotted versus (Figure 6b) concentration of amaranth. Based on the final slope and the Cottrell equation, the mean value of *D* for amaranth was calculated as $6.5\times10^{-5}$ cm$^2$ s$^{-1}$.

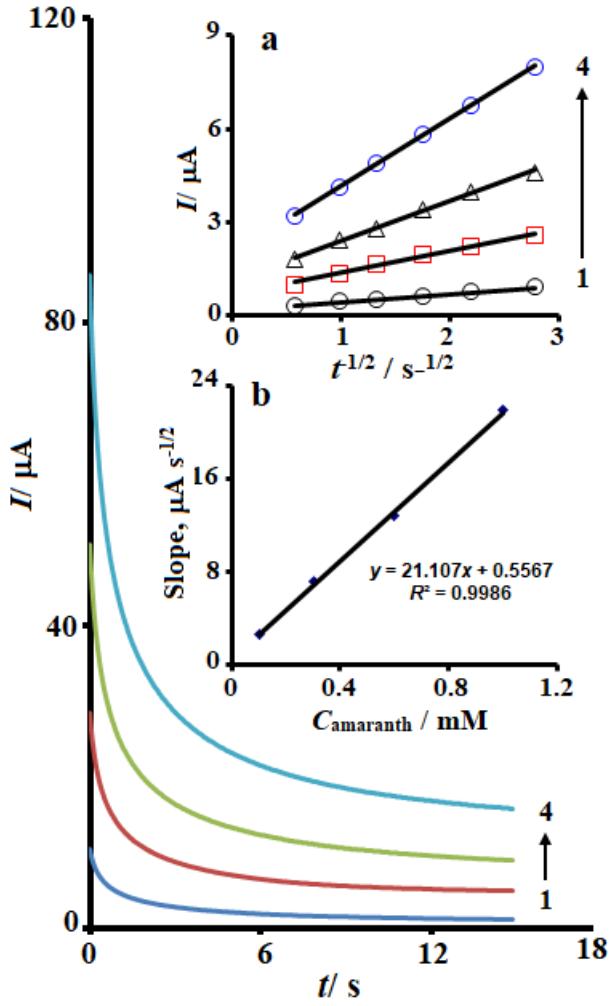


***Figure 6.*** *Chronoamperograms at the AC-$Co_3O_4$-CPE in 0.1 M PBS (pH of 7.0) containing different concentrations of amaranth; 1 to 4 correspond to 0.1, 0.3, 0.6 and 1.0 mM of amaranth. Inset: The plot of I versus $t^{-1/2}$ obtained from the chronoamperograms 1–4 (a), the slope of straight lines against concentration of amaranth (b)*

*Analytical functions*

The obtained results show that the electrooxidation peak current of amaranth at the AC-$Co_3O_4$-CPE surface could be used for measurement of amaranth in solution. Since differential pulse voltammetry (DPV) has a higher sensitivity compared to other quantitative methods, just this method was used to investigate the linear range of the method. The DPV parameters were tested and the best currents were obtained by using (initial potential = 470 mV, end potential = 690 mV, potential = 0.01 V and pulse amplitude = 0.025 V). To perform this study, the AC-$Co_3O_4$-CPE was placed in a series of amaranth solutions with different concentrations and peak current was measured. According to the data (Figure 7), the oxidation current of amaranth at the AC-$Co_3O_4$-CPE surface has a linear dependence on the amaranth concentration (at range 0.1 to 215.0 µM), with a correlation coefficient of 0.9994. Finally, based on $3S_b/m$, a detection limit of 10 nM for amaranth was calculated.

Table 1 compares analytical function of the AC-$Co_3O_4$-CPE with the other modified electrodes [1,3,18-20,34,43,44,46]. As seen in the Table 1, the detection limit and the linear range obtained using the AC-$Co_3O_4$-CPE is in the range of many reports or even better. The high sensitivity may be ascribed to the porous structure of the AC-$Co_3O_4$ nanocomposite, which facilitates the transport of electroactive molecules. The low detection limit may be the result of the synergistic effect of the activated carbon and the $Co_3O_4$ NPs.

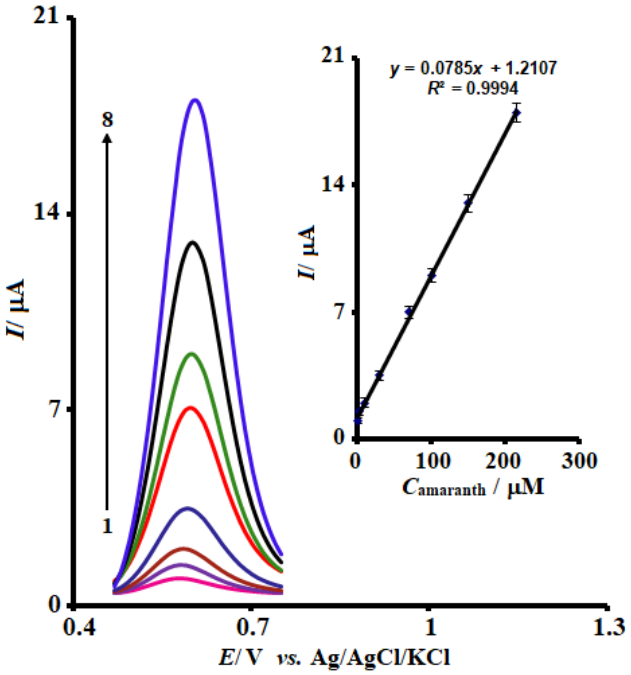


***Figure 7.*** *DPVs of the AC-$Co_3O_4$-CPE in 0.1 M PBS (pH 7.0) containing different concentrations of amaranth (0.1, 2.5, 10.0, 30.0, 70.0, 100.0, 150.0 and 215.0 µM). Inset: the peak current plots versus concentration of amaranth (0.1-215.0 µM)*

***Table 1.*** *Figure of merit of the AC-$Co_3O_4$-CPE compared to other electrodes used in the measurement of amaranth*

| Method | LOD, nM | Linear range, µM | Ref. |
|---|---|---|---|
| GCE modified with electropolymerization of molecularly imprinted polypyrrole film on multiwalled carbon nanotube surface | 0.4 | 0.007-17 | [1] |
| Carbon paste electrode modified with alumina microfibers and accumulation | 0.75 | 0.001-0.15 | [3] |
| Expanded graphite paste electrode | 36 | 0.08-4 | [18] |
| Carbon paste electrode modified with nanostructured resorcinol-formaldehyde carbonized polymers and accumulation | 0.27 | 0.0005-0.1 | [19] |
| Glassy carbon electrode (GCE) modified with Pd-doped polyelectrolyte functionalized graphene | 7 | 0.1-9 | [20] |
| GCE modified with molecularly imprinted electrochemical sensor based on Pd-Cu bimetallic alloy functionalized graphene | 2 | 0.006-10 | [34] |
| GCE modified with porous graphene material-graphene nanomeshes | 0.7 | 0.005-1 | [43] |
| GCE modified with manganese dioxide Nanorods/electrochemically reduced graphene oxide nanocomposites | 1 | 0.02-400 | [44] |
| GCE modified with functionalized graphene oxide/chitosan/ionic liquid nanocomposite supported nanoporous gold | 37.3 | 0.008-1.2 | [46] |
| AC-$Co_3O_4$-CPE | 10.0 | 0.1-215.0 | This work |

*Repeatability, reproducibility and stability*

To evaluate the reproducibility of the AC-$Co_3O_4$-CPE sensor, DPV was used. The calculated RSD for five measurements of 100 µM of amaranth at five different electrodes prepared in the same way was 3.4 %, which demonstrates reasonable reproducibility of the AC-$Co_3O_4$-CPE sensor. Also, the relative standard deviation (RSD) of six repeated determinations of 100.0 µM of amaranth with one electrode was 3.7 % which demonstrates reasonable repeatability of the AC-$Co_3O_4$-CPE sensor. To assess stability of the AC-$Co_3O_4$-CPE sensor, a modified electrode was stored for three weeks, and then used for amaranth determination. The obtained data showed that current response of the

AC-$Co_3O_4$-CPE sensor to the amaranth after 3 weeks was 94.5 % of its initial value, which illustrates a very good sensor stability.

*Interference effect*

In the analytical chemistry, the selectivity of sensor is a very important factor. For this assesses, the effect of some annoying species on the measurement of 50.0 µM amaranth was assessed by DPV under optimum conditions. The possible interfering species were selected in such a way that they could be present in the real samples. The obtained data showed that 50-fold lemon yellow, sunset yellow, rhodamine B, glucose, ascorbic acid and citric acid, show no disturbance in the measurement of amaranth and the change in $I_p$ due to interfere was less than 5 %. Therefore, can be said that the electrode has a good selectivity.

*Real-sample analysis*

Artificial colors are often used as brightening agent to add in soft drinks for better appearance and taste, and therefore we chose soft drinks as real samples to determine amaranth. For this purpose, the applicability of the AC-$Co_3O_4$-CPE in determining the true samples, the pre-prepared samples were transferred to electrochemical cell and the amount of amaranth was measured using DPV. The standard addition method was used to increase the accuracy of the measurement. The results were given in Table 2 and showed that the recovery percentages were in the range of 98.2 to 103.4 %. Also, the RSD percentages of the method were 3.6 % or less, which indicates the high reliability of the AC-$Co_3O_4$-CPE in real samples.

***Table 2.*** *Application of the AC-$Co_3O_4$-CPE to detect amaranth in real samples (n = 5)*

| Sample | $C_{amaranth}$ / µM | | Recovery, % | RSD, % |
|---|---|---|---|---|
| | Spiked* | Found** | | |
| Grape soda | 0.21 | 0.56±0.03 | --- | 3.3 |
| | 5.0 | 5.63±0.18 | 101.4 | 3.6 |
| | 10.0 | 10.41±0.34 | 98.5 | 3.3 |
| | 20.0 | 20.92±0.64 | 101.8 | 3.2 |
| Lemon soda | --- | ND* | --- | --- |
| | 5.0 | 5.17±0.21 | 103.4 | 3.5 |
| | 10.0 | 10.32±0.38 | 103.2 | 3.2 |
| | 20.0 | 19.64±0.66 | 98.2 | 3.3 |

*The added standard to the sample, **The amount of amaranth that was determined, ***Not detected

## Conclusions

In this research, a new modified CPE was constructed for the measurement of amaranth. Due to modification of the electrode surface using AC-$Co_3O_4$-CPE nanocomposite, the electrode response to amaranth increased and thus the sensitivity of the measurement increased too. The AC-$Co_3O_4$-CPE was successfully applied for the measurement of amaranth in soft drinks samples. Simplicity, portability and cost-effectiveness are some of the advantages of the developed AC-$Co_3O_4$-CPE.

## Conflict of interest

Authors declare that there is no conflict of interest related to publishing of the present work.

## References

[1] Y. Wu, G. Li, Y. Tian, J. Feng, J. Xiao, J. Liu, X. Liu, Q. He, Electropolymerization of molecularly imprinted polypyrrole film on multiwalled carbon nanotube surface for highly selective and stable determination of carcinogenic amaranth, *Journal of Electroanalytical Chemistry* **895** (2021) 115494. https://doi.org/10.1016/j.jelechem.2021.115494

[2] Y. Xie, Y. Li, L. I. Niu, H. Wang, H. E. Qian, W. Yao, A novel surface-enhanced Raman scattering sensor to detect prohibited colorants in food by graphene/silver nanocomposite, *Talanta* **100** (2012) 32-37. https://doi.org/10.1016/j.talanta.2012.07.080
[3] Y. Zhang, T. Gan, C. Wan, K. Wu, Morphology-controlled electrochemical sensing amaranth at nanomolar levels using alumina, *Analytica Chimica Acta* **764** (2013) 53-58. http://dx.doi.org/10.1016/j.aca.2012.12.020
[4] P. Mpountoukas, A. Pantazaki, E. Kostareli, P. Christodoulou, D. Kareli, S. Poliliou, C. Mourelatos, V. Lambropoulou, T. Lialiaris, Cytogenetic evaluation and DNA interaction studies of the food colorants amaranth, erythrosine and tartrazine, *Food and Chemical Toxicology* **48** (2010) 2934-2944. https://doi.org/10.1016/j.fct.2010.07.030
[5] V. K. Gupta, R. Jain, A. Mittal, T. A. Saleh, A. Nayak, S. Agarwal, S. Sikarwar, Photocatalytic degradation of toxic dye amaranth on $TiO_2$/UV in aqueous suspensions, *Materials Science and Engineering C* **32** (2012) 12-17. https://doi.org/10.1016/j.msec.2011.08.018
[6] A. Basu, G. S. Kumar, Interaction of toxic azo dyes with heme protein: Biophysical insights into the binding aspect of the food additive amaranth with human hemoglobin, *Journal of Hazardous Materials* **289** (2015) 204-209. https://doi.org/10.1016/j.jhazmat.2015.02.044
[7] W. R. P. Barros, J. R. Steter, M. R. V. Lanza, A. J. Motheo, Degradation of amaranth dye in alkaline medium by ultrasonic cavitation coupled with electrochemical oxidation using a boron-doped diamond anode, *Electrochimica Acta* **143** (2014) 180-187. https://doi.org/10.1016/j.electacta.2014.07.141
[8] K. Rovina, S. Siddiquee, S. M. Shaarani, Toxicology, extraction and analytical methods for determination of amaranth in food and beverage products, *Trends in Food Science and Technology* **65** (2017) 68-79. http://dx.doi.org/10.1016/j.tifs.2017.05.008
[9] Y. Perdomo, V. Arancibia, O. García-Beltrán, E. Nagles, Adsorptive stripping voltammetric determination of amaranth and tartrazine in drinks and gelatins using a screen-printed carbon electrode, *Sensors* **17** (2017) 2665. https://doi.org/10.3390/s17112665
[10] F. I. de Andrade, M. I. Florindo Guedes, I. G. Pinto Vieira, F. N. Pereira Mendes, P. A. Salmito Rodrigues, C. S. Costa Maia, M. M. Marques Avila, L. D. M. Ribeiro, Determination of synthetic food dyes in commercial soft drinks by TLC and ion-pair HPLC, *Food Chemistry* **157** (2014) 193-198. https://doi.org/10.1016/j.foodchem.2014.01.100
[11] Y. Shen, X. Zhang, W. Prinyawiwatkul, Z. Xu, Simultaneous determination of red and yellow artificial food colourants and carotenoid pigments in food products, *Food Chemistry* **157** (2014) 553. https://doi.org/10.1016/j.foodchem.2014.02.039
[12] X. Q. Li, Q. H. Zhang, K. Ma, H. M. Li, Z. Guo, Identification and determination of 34 water-soluble synthetic dyes in foodstuff by high performance liquid chromatography-diode array detection-ion trap time-of-flight tandem mass spectrometry, *Food Chemistry* **182** (2015) 316-326. https://doi.org/10.1016/j.foodchem.2015.03.019
[13] C.-F. Tsai, C.-H. Kuo, D. Y.-C. Shih, Determination of 20 synthetic dyes in chili powders and syrup-preserved fruits by liquid chromatography/tandem mass spectrometry, *Journal of Food and Drug Analysis* **23** (2015) 453-462. https://doi.org/10.1016/j.jfda.2014.09.003
[14] F. Martin, J.-M. Oberson, M. Meschiari, C. Munari, Determination of 18 water-soluble artificial dyes by LC-MS in selected matrices, *Food Chemistry* **197** (2016) 1249-1255. https://doi.org/10.1016/j.foodchem.2015.11.067
[15] N. Elizabeth Llamas, M. Garrido, M. Susana Di Nezio, B. S. Fernandez Band, Second order advantage in the determination of amaranth, sunset yellow FCF and tartrazine by UV-vis and multivariate curve resolution-alternating least squares, *Analytica Chimica Acta* **655** (2009) 38-42. https://doi.org/10.1016/j.aca.2009.10.001
[16] O. Sha, X. Zhu, Y. Feng, W. Ma, Aqueous two-phase based on ionic liquid liquid-liquid microextraction for simultaneous determination of five synthetic food colourants in

different food samples by high-performance liquid chromatography, *Food Chemistry* **174** (2015) 380-386. https://doi.org/10.1016/j.foodchem.2014.11.068

[17] Y. Ni, J. Bai, Simultaneous determination of amaranth and Sunset Yellow by ratio derivative voltammetry, *Talanta* **44** (1997) 105-109. https://doi.org/10.1016/S0039-9140(96)02028-0

[18] J. Zhang, M. Wang, C. Shentu, W. Wang, Z. Chen, Simultaneous determination of the isomers of Ponceau 4R and amaranth using an expanded graphite paste electrode, *Food Chemistry* **160** (2014) 11-15. http://dx.doi.org/10.1016/j.foodchem.2014.03.078

[19] L. Ji, Y. Zhang, S. Yu, S. Hu, K. Wu, Morphology-tuned preparation of nanostructured resorcinol-formaldehyde carbonized polymers as highly sensitive electrochemical sensor for amaranth, *Journal of Electroanalytical Chemistry* **779** (2016) 169-175. http://dx.doi.org/10.1016/j.jelechem.2016.03.011

[20] Y. Gao, L. Wang, Y. Zhanga, L. Zoua, G. Lia, B. Yea, Electrochemical behavior of amaranth and its sensitive determination based on Pd-doped polyelectrolyte functionalized graphene modified electrode, *Talanta* **168** (2017) 146-151. http://dx.doi.org/10.1016/j.talanta.2017.03.035

[21] J. ShaSha, Z. Huijun, Z. Li, Q. LingBo, Y. LanLan, electrochemical sensor based on poly(sodium 4-styrenesulfonate) functionalized graphene and $Co_3O_4$ nanoparticle clusters for detection of amaranth in soft drinks, *Food Analytical Methods* **10** (2017) 3149-3157. http://dx.doi.org/10.1007/s12161-017-0889-z

[22] S. Z. Mohammadi, H. Beitollahi, T. Rohani, H. Allahabadi, S. Tajik, $La_2O_3/Co_3O_4$ nanocomposite modified screen printed electrode for voltammetric determination of sertraline, *Journal of the Serbian Chemical Society* **85** (2020) 505-515. https://doi.org/10.2298/JSC190326126M

[23] S. Tajik, Z. Dourandish, K. Zhang, H. Beitollahi, Q.V. Le, H.W. Jang, M. Shokouhimehr, Carbon and graphene quantum dots: a review on syntheses, characterization, biological and sensing applications for neurotransmitter determination, *RSC Advances* **10** (2020) 15406-15429. https://doi.org/10.1039/D0RA00799D

[24] H. Beitollahi, S. Z. Mohammadi, S. Tajik, Electrochemical behavior of Morphine at the surface of magnetic core shell manganese ferrite nanoparticles modified screen printed electrode and its determination in real samples, *International Journal of Nano Dimensions* **10** (2019) 304-312. https://journals.iau.ir/article_662362_9f15b5034a739a32f6fe497715b93a47.pdf

[25] S. Z. Mohammadi, H. Beitollahi, E. Bani Asadi, Electrochemical determination of hydrazine using a $ZrO_2$ nanoparticles-modified carbon paste electrode. *Environmental Monitoring and Assessment* **187** (2015) 122. https://doi.org/10.1007/s10661-015-4309-9

[26] S. Z. Mohammadi, H. Beitollahi, M. Kaykhaii, N. Mohammadizadeh, S. Tajik, R. Hosseinzadeh, Simultaneous determination of droxidopa and carbidopa by carbon paste electrode functionalized with $NiFe_2O_4$ nanoparticle and 2-(4-ferrocenyl-[1,2,3]triazol-1-yl)-1-(naphthalen-2-yl) ethenone, *Measurement* **155** (2020) 107522 https://doi.org/10.1016/j.measurement.2020.107522

[27] S. Tajik, H. Beitollahi, P. Biparva, Methyldopa electrochemical sensor based on a glassy carbon electrode modified with $Cu/TiO_2$ nanocomposite, *Journal of the Serbian Chemical Society* **83** (2018) 863-874. https://doi.org/10.2298/JSC170930024T

[28] S. Z. Mohammadi, Hadi Beitollahi, M. Askari, R. Hosseinzadeh, Application of a modified carbon paste electrode using core–shell magnetic nanoparticle and modifier for simultaneous determination of norepinephrine, acetaminophen and tryptophan, *Russian Journal of Electrochemistry* **57** (2021) 74-84. https://doi.org/10.1134/S1023193521010079

[29] S. Esfandiari Baghbamidi, H. Beitollahi, S. Tajik, R. Hosseinzadeh, Voltammetric sensor based on 1-benzyl-4-ferrocenyl-1h- [1,2,3]-triazole /carbon nanotube modified glassy

carbon electrode; detection of hydrochlorothiazide in the presence of propranolol, *International Journal of Electrochemical Science* **11** (2016) 10874-10883. https://doi.org/10.20964/2016.12.92

[30] S. Z. Mohammadi, H. Beitollahi, H. Allahabadi, T. Rohani, Disposable electrochemical sensor based on modified screen-printed electrode for sensitive cabergoline quantification, *Journal of Electroanalytical Chemistry* **847** (2019) 113223. https://doi.org/10.1016/j.jelechem.2019.113223

[31] S. Z. Mohammadi, M. Dadkhodazadeh, T. Rohani, A novel multicomponent TMDC, $MoS_2$–$WS_2$–$CoS_x$, as an effective electrocatalyst for simultaneous detection ultra-levels of prednisolone and rutin in human body fluids, *Microchemical Journal* **164** (2021) 106019. https://doi.org/10.1016/j.microc.2021.106019

[32] S. Z. Mohammadi, H. Beitollahi, M. Kaykhaii, N. Mohammadizadeh, A novel electrochemical sensor based on graphene oxide nanosheets and ionic liquid binder for differential pulse voltammetric determination of droxidopa in pharmaceutical and urine samples, *Russian Journal of Electrochemistry* **55** (2019) 1229-1236. https://doi.org/10.1134/S1023193519120127

[33] S. Z. Mohammadi, S. Tajik, H. Beitollahi, Screen printed carbon electrode modified with magnetic core shell manganese ferrite nanoparticles for electrochemical detection of amlodipine, *Journal of the Serbian Chemical Society* **84** (2019) 1005-1016. https://doi.org/10.2298/JSC1810056036M

[34] L. Li, H. Zheng, L. Guo, L. Qu, L. Yu, A sensitive and selective molecularly imprinted electrochemical sensor based on Pd-Cu bimetallic alloy functionalized graphene for detection of amaranth in soft drink, *Talanta* **197** (2019) 68–76. https://doi.org/10.1016/j.talanta.2019.01.009

[35] S. Tvorynska, B. Josypčuk, J. Barek, L. Dubenska, Electrochemical behavior and sensitive methods of the voltammetric determination of food azo dyes amaranth and allura red AC on amalgam electrodes, *Food Analytical Methods* **12** (2018) 409-421. https://doi.org/10.1007/s12161-018-1372-1

[36] J.-L. He, W. Kou, C. Li, J.-J. Cai, F.-Y. Kong, W. Wang, Electrochemical sensor based on single-walled carbon nanotube-TiN nannocomposites for detecting amaranth , *International Journal of Electrochemical Science* **10** (2015) 10074-10082. http://www.electrochemsci.org/papers/vol10/101210074.pdf

[37] M. Sheikhshoaie, H. Karimi-Maleh, I. Sheikhshoaie, M. Ranjbar, Voltammetric amplified sensor employing $RuO_2$ nano-road and room temperature ionic liquid for amaranth analysis in food samples, *Journal of Molecular Liquids* **229** (2017) 489-494. https://doi.org/10.1016/j.molliq.2016.12.088

[38] J. A. Buledi, A. R.Solangi, A. Hyder, N. H. Khand, S. A. Memon, A. Mallah, N. Mahar, E. N. Dragoi, P. Show, M. Behzadpour, H. Karimi-Maleh, Selective oxidation of amaranth dye in soft drinks through tin oxide decorated reduced graphene oxide nanocomposite based electrochemical sensor, *Food and Chemical Toxicology* **165** (2022) 113177. https://doi.org/10.1016/j.fct.2022.113177

[39] H. Beitollahi, F. Garakani Nejad, Z. Dourandish, S. Tajik, A novel voltammetric amaranth sensor based on screen printed electrode modified with polypyrrole nanotubes, *Environmental Research* **214** (2022) 113725. https://doi.org/10.1016/j.envres.2022.113725

[40] P. Mohammadzadeh Jahani, M. R. Aflatoonian, R. Abbasi Rayeni, A. D. Bartolomeo, S. Z. Mohammadi, Graphite carbon nitride-modified screen-printed electrode as a highly sensitive and selective sensor for detection of amaranth, *Food and Chemical Toxicology* **163** (2022) 112962. https://doi.org/10.1016/j.fct.2022.112962

[41] S. Z. Mohammadi, N. Mofidinasab, M. A. Karimi, A. Beheshti, Removal of methylene blue and Cd(II) by magnetic activated carbon–cobalt nanoparticles and its application to wastewater purification, *International Journal of Environmental Science and Technology* **17** (2020) 4815. https://doi.org/10.1007/s13762-020-02767-0

[42] S.Z. Mohammadi, Z. Darijani, Z., M.A. Karimi, Fast and efficient removal of phenol by magnetic activated carbon cobalt nanoparticles, *Journal of Alloys and Compounds* **832** (2020) 154942. https://doi.org/10.1016/j.jallcom.2020.154942

[43] M. Wang, M. Cui, M. Zhao, H. Cao, Sensitive determination of amaranth in foods using graphene nanomeshes, *Journal of Electroanalytical Chemistry* **809** (2018) 117-124. https://doi.org/10.1016/j.jelechem.2017.12.059

[44] Q. He, J. Liu, X. Liu, G. Li, P. Deng, J. Liang, Manganese dioxide nanorods/electrochemically reduced graphene oxide nanocomposites modified electrodes for cost-effective and ultrasensitive detection of amaranth, *Colloids and Surfaces B* **172** (2018) 565-572. https://doi.org/10.1016/j.colsurfb.2018.09.005

[45] A. J. Bard, L. R. Faulkner, *Electrochemical Methods: Fundamentals and Applications*, 2nd edition, Wiley, New York, 2000, pp. 100-137. ISBN: 978-0-471-04372-0

[46] Q. Zhang, W. Cheng, D. Wu, Y. Yang, X. Feng, C. Gao, L. Meng, X. Shen, Y. Zhang, X. Tang, An electrochemical method for determination of amaranth in drinks using functionalized graphene oxide/chitosan/ionic liquid nanocomposite supported nanoporous gold, *Food Chemistry* **367** (2022) 130727. https://doi.org/10.1016/j.foodchem.2021.130727